THE JOURNAL OF PHYSICAL CHEMISTRY A

Article

Cite This: J. Phys. Chem. A 2019, 123, 2592−2600

pubs.acs.org/JPCA

Unraveling the Excited-State Dynamics of Eosin Y Photosensitizers Using Single-Molecule Spectroscopy

Published as part of The Journal of Physical Chemistry virtual special issue "Young Scientists".

Pauline G. Lynch, Huw Richards, and Kristin L. Wustholz*

College of William and Mary, Department of Chemistry, P.O. Box 8795, Williamsburg, Virginia 23187, United States

Supporting Information

ABSTRACT: The intersystem crossing and dispersive electron-transfer dynamics of eosin Y (EY) photosensitizers are probed using single-molecule microscopy. The blinking dynamics of EY on glass are quantified by constructing cumulative distribution functions of emissive ("on") and nonemissive ("off") events. Maximum likelihood estimation (MLE) and goodness-of-fit tests based on the Kolmogorov−Smirnov (KS) statistic are used to establish the best fit to the blinking data and differentiate among competitive photophysical processes. The on-time probability distributions for EY in N_2 and air are power-law distributed after ∼1 s, with fit parameters that are significantly modified upon exposure to oxygen. By extending the statistically principled MLE/KS approach to include an onset time for log-normal behavior, we demonstrate that the off-time distribution for EY in N_2 is best fit to a combination of exponential and log-normal functions. The corresponding distribution for EY in air is best fit to a log-normal function alone. Furthermore, power law and log-normal distributions are observed for an *individual* molecule in air, consistent with dynamic fluctuations in the rate constant for dark-state population and depopulation. These observations support the interpretation that dispersive electron transfer (i.e., the Albery model) from the first excited singlet state (S_1) of EY to trap states on glass is predominately responsible for blinking in oxic conditions. In anoxic environment, both triplet-state blinking and dispersive electron transfer from S_1 and the excited triplet state (T_1) contribute to the excited-state dynamics of EY.

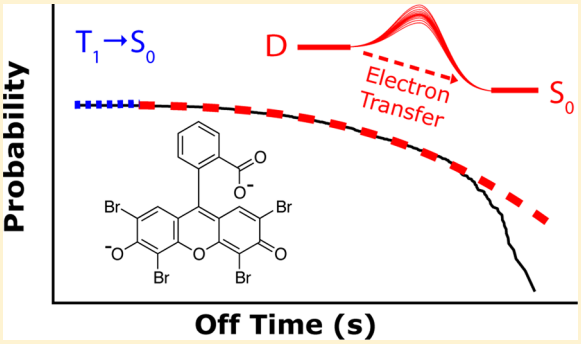

INTRODUCTION

As global energy demand and atmospheric CO_2 levels continue to escalate, there is an urgent need for low-cost, sustainable, and carbon-neutral energy.[1,2] Dye-sensitized photocatalysis (DSP) is a promising method to meet surging energy demands via the direct conversion of solar energy to renewable fuels such as H_2.[3−5] In this approach, a photosensitizer that undergoes fast photoinduced charge generation (i.e., on ps-ns time scales) is coupled to an electrocatalyst for fuel production, which occurs on relatively slow time scales (i.e., ms-s). One strategy to minimize charge recombination losses and kinetic redundancy in DSP is to prolong the lifetime of charge carriers by enhancing intersystem crossing (ISC) to a long-lived triplet excited state that precludes electron injection.[5−7] For example, the photosensitizer eosin Y (EY), a brominated derivative of fluorescein, has been widely used in photocatalytic water splitting[7−13] and photoredox synthesis.[14,15] Though EY demonstrates promise as a photosensitizer for DSP, minimizing kinetic redundancy requires understanding the extent and origin of kinetic dispersion in the electron injection, recombination, and ISC dynamics.

Heterogeneous excited-state dynamics in complex, condensed phase systems can be deciphered using single-molecule spectroscopy.[16−26] For example, single-molecule blinking dynamics (i.e., fluctuations in emission intensities under continuous photoexcitation) have been used to probe the static and dynamic inhomogeneities of the electron-transfer dynamics occurring in dye-sensitized TiO_2.[20−26] To understand the underlying photophysics, the distributions of emissive and nonemissive events (i.e., on and off times, respectively) must be examined using a statistically robust method. A combined maximum likelihood estimation (MLE) and Kolmogorov-Smirnov (KS) test approach is increasingly applied to single-molecule blinking data, as it provides for a more accurate determination of functional form and corresponding fit parameters as compared to standard least-squares fitting.[25−29] For example, previous single-molecule studies have deployed MLE/KS analysis to reveal log-normal distributions for rhodamine dyes on TiO_2, consistent with the Albery model for dispersive electron transfer (i.e., where activation barriers are normally distributed).[25,26,30] More recently, perylenediimide dyes embedded in poly(methyl methacrylate) (PMMA) were

Received: January 14, 2019
Revised: March 1, 2019
Published: March 5, 2019

DOI: 10.1021/acs.jpca.9b00409
J. Phys. Chem. A 2019, 123, 2592−2600

found to exhibit Weibull distributions, consistent with radical ion pair ISC via charge hopping.[31]

Here, we use single-molecule spectroscopy to probe the complex excited-state dynamics of EY photosensitizers immobilized on glass. By extending the MLE/KS methodology to include an onset time for log-normal behavior, competitive photophysical processes can be readily identified. Overall, significant differences in single-molecule emission behavior (i.e., in terms of event rate, photophysical distribution, and photostability) are observed for EY in the presence and absence of oxygen. The off-time distribution of EY in anoxic conditions is best fit to a combination of exponential and log-normal functions, consistent with a kinetic model that incorporates both triplet-state decay and dispersive electron transfer. The observation of log-normally distributed off times in air is consistent with rapid quenching of the excited triplet state by oxygen, such that dispersive electron transfer from the excited singlet state of EY to trap states in glass is predominately responsible for blinking. Furthermore, both static and dynamic heterogeneity of the electron-transfer process is observed, consistent with the observation of dispersive kinetics in an *individual molecule* of EY in air. Ultimately, elucidating the heterogeneous excited-state dynamics and corresponding photostability of EY is relevant to the design of next-generation materials for DSP as well as a range of applications from photodynamic therapy[32,33] to cultural heritage research (e.g., Van Gogh's use of eosin lake).[34−36]

EXPERIMENTAL SECTION

Sample Preparation. EY (~99%) was used as received from Sigma-Aldrich. Ethanol (absolute anhydrous, 200 proof) was obtained from Pharmco-Aaaper. Glass coverslips (Fisher Scientific, 12-545-102) were cleaned in a base bath for 12−24 h, rinsed in deionized water (ThermoScientific, EasyPure II, 18.2 MΩ cm), and dried with clean air (Wilkerson, X06-02-000). All dye solutions were prepared in ethanol using base-bathed glassware. For single-molecule measurements, samples were prepared by spin-coating 35 μL of a 5×10^{-10} M EY solution onto a clean glass coverslip using a spin coater (Laurell Technologies, WS-400−6NPP-LITE) operating at 3000 rpm. The resulting samples were mounted in a custom-designed flow cell and left open to ambient air (i.e., $\rho_{O_2} \approx 160$ Torr) for oxic conditions or continuously flushed with N_2 (Airgas, 100%) at a rate of 0.2−0.5 scfh (Key Instruments, MR3A01AVVT) during anoxic experiments.

Single-Molecule Microscopy and Data Analysis. Samples for single-molecule studies were placed on a nanopositioning stage (Physik Instrumente, LP E-545) on top of a confocal microscope (Nikon, TiU). Laser excitation at 532 nm (Spectra Physics, Excelsior) was focused to a diffraction-limited spot using a high numerical aperture (NA) 100× oil-immersion objective (Nikon Plan Fluor, NA = 1.3). An excitation power (P_{exc}) of 0.37 μW at the sample was used for single-molecule measurements. Emission from the sample was collected through the objective, spectrally filtered using an edge filter (Semrock, LP03−532RS-2S), and focused to an avalanche photodiode detector (APD) with a 50 μm aperture (MPD, PDM050CTB) to provide for confocal resolution. A *z*-axis microscope lock (Applied Science Instruments, MFC-2000) was used to maintain the focal plane of the objective during raster scans. A custom LabView program was used to control the nanopositioning stage and collect corresponding emission intensity using a 30 ms dwell time. Single-molecule emission was established based on the observation of diffraction-limited spots, blinking dynamics, irreversible single-step photobleaching, and concentration dependence of the spot density. The spot density was approximately five molecules per 36 μm^2 for 5×10^{-10} M EY in N_2 and air.

Blinking dynamics were acquired using a 10 ms integration time for at least 200 s and analyzed using the change-point detection (CPD) method as described in detail elsewhere.[37] Previous studies have shown that using a simple threshold to distinguish on and off events is problematic and that CPD provides for a more accurate determination of the true number and intensity of states that are accessible to the system.[38−41] CPD reports the statistically-significant intensities and corresponding temporal durations for up to 20 distinct intensity levels. In addition to resolving multiple emissive intensities, CPD also provides the ability to differentiate two types of events: segments and intervals. Segments correspond to the temporal duration of an event at a particular intensity. Intervals are composed of successive segments that occur prior to a switch (i.e., between on and off), with each single molecule exhibiting an equal number of on and off intervals. Consistent with previous reports,[25,26] we use the general terms "times" and "events" to refer to segments. In CPD analysis, the first and last events in a blinking trace are disregarded, since they are artificially set by the observation window. The lowest deconvolved intensity level is designated as a nonemissive (off) or photobleaching event, depending on whether or not emission is recovered. Levels with intensities greater than one standard deviation above the root-mean-square (rms) noise (i.e., about 4 counts per 10 ms) are denoted as emissive (on). The single-molecule event rate is defined as the total number of events recorded during the observation period.

Following CPD analysis, the resulting on- and off-time distributions are converted into complementary cumulative distribution functions (i.e., CCDFs) that describe the probability of an event occurring in a time greater than or equal to t according to $\mathrm{CCDF} = 1 - \frac{1}{N}\sum_i t_i \leq t$.[27] The fit parameters and corresponding goodness-of-fit of the experimental CCDFs relative to the proposed functions (i.e., power law, Weibull, and log-normal) are quantified using MLE and the KS statistic (i.e., *p*-value) as previously described.[25−29] Since analytical expressions for the fit parameters of the log-normal distribution with onset time cannot be determined using MLE, a numerical method was used to refine these values. In this approach, an initial guess for the mean of the distribution is used to seed the numerical method, and the best fit is determined by the set of parameters that minimizes the KS statistic. Standard errors in the fit parameters are determined from the second derivative of the log-likelihood with respect to the parameters. For clarity, we use the term probability distribution for CCDF throughout this paper. All data analyses and fitting procedures were completed in Matlab (version R2018a).

RESULTS

Blinking Statistics of Eosin Y in Anoxic Environment. A single-molecule confocal microscope employing continuous laser excitation at 532 nm was used to characterize the photophysics of single EY molecules adsorbed onto glass and in an anoxic environment. Figure 1 presents a typical single-molecule data set, consisting of a false-colored image the fluorescence from 5×10^{-10} M EY spun coat on glass and a

DOI: 10.1021/acs.jpca.9b00409
J. Phys. Chem. A 2019, 123, 2592−2600

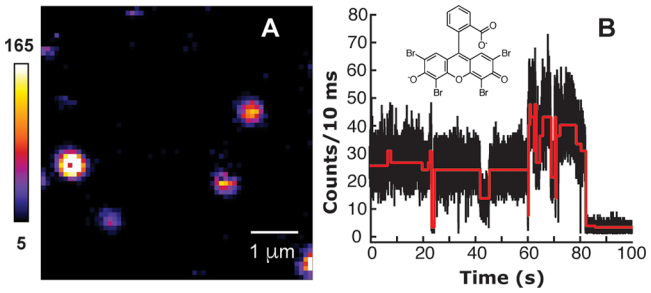

Figure 1. Representative single-molecule data for EY in N_2. (A) False-colored $6 \times 6\ \mu m^2$ image of the fluorescence from 5×10^{-10} M EY in N_2, obtained using 532 nm excitation. Color scale corresponds to counts per 30 ms. (B) 100 s excerpt of the blinking dynamics for an individual EY molecule. The fluorescence intensity trajectory (black line) is recorded using a 10 ms integration time. Analysis of the blinking dynamics with CPD demonstrates that 14 statistically significant intensities and 26 distinct events are observed (red line).

representative single-molecule emission-time trace (i.e., blinking dynamics). Analysis of the blinking dynamics using the CPD method demonstrates that 14 distinct intensity levels, 24 on events, and 2 off events are detected, with an average event rate of 0.13 s^{-1}. Blinking dynamics are observed until the photobleaching event occurs at 85.9 s. The observation that the blinking dynamics of EY demonstrate multiple emissive intensities prior to photobleaching is consistent with prior single-molecule studies of xanthene and anthraquinone dyes on glass.[26,29]

To determine the range of photophysical behavior demonstrated by EY, the blinking dynamics of 127 molecules were measured, compiled, and quantified in terms of on- and off-time probability distributions (i.e., CCDFs) and event rate. Figure 2 presents the resulting on-time probability distribution that contains 1872 events, with an average on time of 3.5 s and individual values that range from 0.02 to 151.66 s. The corresponding off-time probability distribution contains 513 events, with individual values ranging from 0.04 to 195.62 s and an average off time of 17.15 s. The average off time is much longer than the reported triplet lifetime of EY (e.g., 55 μs in water,[42] 3.6 ms in PMMA,[43] and 1 ms on alumina[44]) indicating that triplet-state decay is not the predominant mechanism responsible for blinking. The average single-molecule event rate is 0.09 ± 0.01 s^{-1} $molecule^{-1}$, with the error corresponding to the standard deviation of the mean. Finally, of 127 EY molecules, 87 (69%) underwent single-step photobleaching within the 200 s observation period. To probe the nature of the nonemissive state, the on- and off-time probability distributions were fit to several test functions that connect to different kinetic models. For example, if blinking is due to the population and depopulation of the triplet state of EY, consistent with first-order kinetics, the on and off times will be exponentially distributed. However, the probability distributions in Figure 2 are not well-described by exponential functions, motivating us to consider more complex photophysics and corresponding test functions (e.g., the power law).

To identify the functional form of the probability distributions, the compiled blinking data were fit to power-law, Weibull, and log-normal functions using the statistically robust MLE/KS method.[25−29] In this approach, the power law (i.e., $P(t) = At^{-\alpha}$) is normalized from an onset time for power-law behavior (t_{min}) to give:

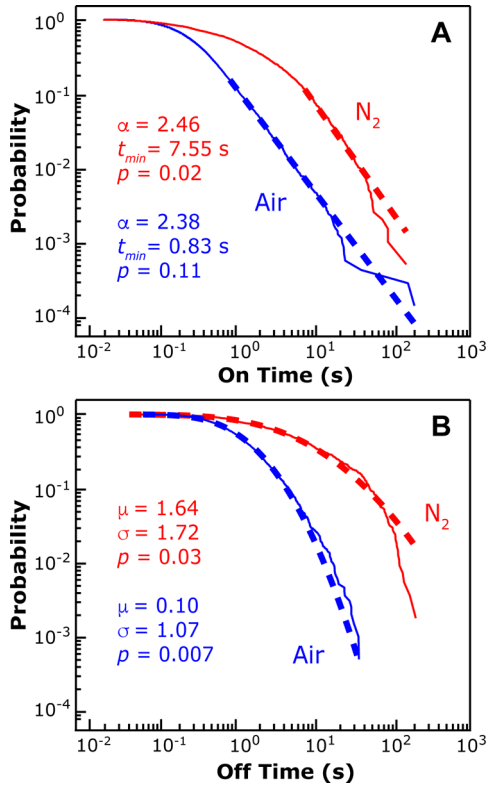

Figure 2. On- and off-time probability distributions (solid lines) for EY on glass in N_2 (red) and air (blue). (A) On times are shown with best fit to a subset of the data by power laws (dashed lines). (B) Off times are best fit to log-normal functions (dashed lines). The log-normal fit parameters are significantly modified in air relative to N_2.

$$P(t) = \frac{\alpha - 1}{t_{min}}\left(\frac{t}{t_{min}}\right)^{-\alpha}, \quad \alpha > 1 \tag{1}$$

A combination of MLE and KS tests are used to establish the best-fit parameters (i.e., α and t_{min}), and goodness-of-fit is determined using a KS test, which quantifies the distance between the empirical data and hypothesized model in a p-value. Here, the probability that the data match the model is increased as the p-value approaches unity, and p-values <0.05 indicate that the model has less than a 5% probability of being the true distribution.[27,28]

The results of the combined MLE/KS analysis of the on- and off-time probability distributions for EY in N_2 are presented in Table 1. According to the goodness-of-fit (i.e., p-values) alone, the on-time distribution is best fit to a power law with $\alpha = 2.46 \pm 0.03$ and $p = 0.02$. Attempts to fit the on-time data to Weibull and log-normal functions produce p-values that are equal to zero. Although the observation of a positive p-value supports the power-law model, the calculated t_{min} value of 7.55 s means that the power law is only operative for a small subset (4%) of on times (Figure 2). Ultimately, MLE/KS analysis demonstrates that the on-time probability distribution is best fit to a power law above an onset time of ~10^1 s, but for a majority of the data the power-law function is inoperative.

The off-time probability distribution for EY in N_2 is best fit to a power law with $\alpha = 6.7 \pm 0.3$, $t_{min} = 107.43$ s, and $p = 0.74$. However, similar to the case for the on-time data, the power law is not valid for the vast majority (98%) of the blinking data. Instead, a log-normal distribution most closely represents the complete off-time data as evidenced by a p-value of 0.03 as

DOI: 10.1021/acs.jpca.9b00409
J. Phys. Chem. A 2019, 123, 2592−2600

Table 1. Best-Fit Parameters and *p*-Values for Power-Law, Weibull, and Lognormal Distributions[a]

		power law: $\frac{\alpha-1}{t_{min}}\left(\frac{t}{t_{min}}\right)^{-\alpha}$			log-normal: $\frac{1}{t\sigma\sqrt{2\pi}}e^{-((\ln(t)-\mu)^2/2\sigma^2)}$			Weibull: $\frac{A}{B}\left(\frac{t}{B}\right)^{A-1}e^{-(t/B)^A}$		
		t_{min} (s)	α	p	μ	σ	p	A	B	p
ON	N_2	7.55	2.46 ± 0.03	0.02	−0.01 ± 0.04	1.66 ± 0.03	0	0.640 ± 0.005	2.31 ± 0.07	0
	air	0.83	2.38 ± 0.02	0.11	−1.17 ± 0.01	1.05 ± 0.01	0	0.820 ± 0.002	0.55 ± 0.01	0
OFF	N_2	107.43	6.7 ± 0.3	0.74	1.64 ± 0.08	1.72 ± 0.05	0.03	0.617 ± 0.008	12.1 ± 0.8	0
	air	4.73	2.83 ± 0.04	0.20	0.10 ± 0.03	1.07 ± 0.02	0.007	0.90 ± 0.01	1.9 ± 0.2	0

[a]Errors represent one standard deviation.

compared to zero for the other functions. The log-normal distribution occurs when the logarithm of the sampled variable (t) is normally distributed according to

$$P(t) = \frac{1}{\sqrt{2\pi}\sigma t}e^{-[(\ln(t)-\mu)^2/2\sigma^2]} \quad (2)$$

where the scale parameters μ and σ correspond to the geometric mean and standard deviation of the variable's natural logarithm, respectively. The off-time probability distribution for EY in N_2 is best fit to a log-normal function corresponding to μ = 1.64 ± 0.08 and σ = 1.72 ± 0.05 (Figure 2).

Overall, applying the CPD and MLE/KS analyses to the blinking data reveals several important observations about the photophysics of EY in N_2. First, blinking dynamics are complex, exhibiting multiple emissive intensities for each molecule. Since EY is immobilized on glass and no evidence for modifications to the transition dipole moment orientation were revealed during successive fluorescence measurements, the observation of multiple emissive intensities is unlikely to originate from orientational fluctuations. For the collection of EY molecules in N_2: on times are power-law distributed after an onset time, and off times are weakly log-normally distributed. These observations are consistent with previous single-molecule studies on glass, which attributed the power-law and log-normal distributions to dispersive electron transfer between dyes and trap states in the glass substrate.[25,26,45,46]

However, in the present case, the observation of statistically insignificant p-values suggests that dispersive electron transfer is not solely responsible for blinking. Previous ensemble-averaged studies have shown that, upon photoexcitation, EY undergoes rapid ISC (i.e., $k_{isc} \approx 1 \times 10^8$ s^{-1}) to its lowest-energy triplet state, which can be long-lived (i.e., >1 ms) on solid substrates.[14,43,44,47] Although the probability of a 1 s off event occurring for a 1 ms triplet lifetime is very small ($\sim 1 \times 10^{-44}$), triplet blinking could still be operative, especially at early times. In this scenario, the off-time probability distribution would contain contributions from two distinct processes: triplet-state decay and dispersive electron transfer. The presence of molecular oxygen is known to play a significant role in the excited-state dynamics of EY through rapid quenching of the triplet state to produce singlet oxygen.[14,32,36,43] Therefore, to examine the possibility that ISC to/from the triplet state contributes to the single-molecule photophysics of EY, we performed blinking measurements in the presence of oxygen.

Impact of Oxygen on Blinking Dynamics. Representative single-molecule data for EY in the presence of oxygen are shown in Figure 3. The false-colored image of the fluorescence from 5×10^{-10} M EY in air (Figure 3A) is pixelated as compared to the corresponding data obtained in N_2 (Figure 1A), demonstrating that nonemissive events with durations that exceed the 30 ms bin time are frequently observed. The blinking dynamics of EY in air are also quite distinct. The molecule in

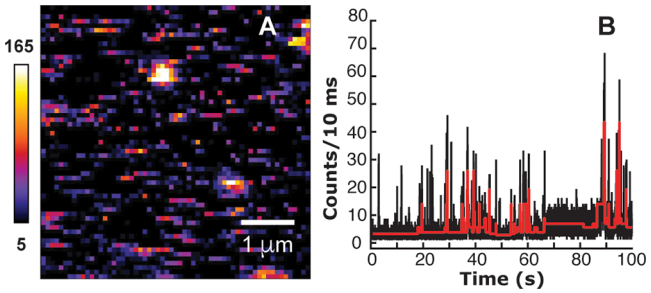

Figure 3. Representative single-molecule data for EY in air. (A) False-colored 6 × 6 μ m^2 fluorescence image of 5×10^{-10} M EY in air, with color scale corresponding to counts per 30 ms. (B) 100 s portion of a single-molecule blinking trace, which contains a total of 11 statistically significant intensities and 149 events according to CPD analysis (red line).

Figure 3B demonstrates 11 distinct intensity levels, 113 on events, 36 off events, and an average event rate of 0.75 s^{-1}. Furthermore, whereas 69% of EY molecules in N_2 underwent photobleaching within 200 s, none in air demonstrated photobleaching within the same time period. Indeed, molecules in air exhibited persistent blinking dynamics for as long as 1000 s (see Figure S1). These observations are consistent with previous ensemble-averaged studies that demonstrated enhanced photostability of EY in oxygen as compared to anoxic conditions.[36]

As a result of these long observation periods and high event rates, the compiled on- and off-time probability distributions for 17 molecules in air (Figure 2) contain thousands of events (i.e., 6681 emissive and 1810 nonemissive events, respectively). Emissive events ranged from 0.02 to 193.07 s in duration, with an average on time of 0.66 s. Corresponding nonemissive events lasting from 0.06 to 36.2 s are observed, with an average off time of 2.0 s. Both the average on and off times are an order of magnitude shorter in air relative to N_2. The average single-molecule event rate of 0.90 ± 0.07 s^{-1} $molecule^{-1}$ is an order of magnitude higher than the event rate measured in N_2.

Table 1 summarizes the MLE/KS fitting results for the on- and off-time probability distributions of EY in air. The on-time probability distribution is well-represented by a power law (i.e., p = 0.11) corresponding to α = 2.38 ± 0.02 and t_{min} = 0.83 s. In this case the power-law model is operative for 31% of the blinking data. Attempts to fit the on-time data to Weibull and log-normal distributions yield p-values that are equal to zero. The off-time probability distribution for EY in air is somewhat fit by a power law with α = 2.83 ± 0.04, t_{min} = 4.73 s, and p = 0.20. However, as in the case for the off-time data for EY in N_2, the power law is only operative for a subset (10%) of the data. The observation of a nonzero p-value of 0.007 suggests that a log-normal distribution with μ = 0.10 ± 0.03 and σ = 1.07 ± 0.02 may be a plausible model for the off-time data.

DOI: 10.1021/acs.jpca.9b00409
J. Phys. Chem. A 2019, 123, 2592−2600

The long observation periods and high event rates for EY in air also provided for the ability to examine the photophysical distributions of individual molecules. Figure S2 presents the on- and off-time probability distributions obtained from a 500 s blinking trace of a single EY molecule in air. The single-molecule event distributions are best fit to power-law and log-normal functions, consistent with the results derived from collections of EY molecules. The single-molecule on-time probability distribution is well-represented (i.e., $p = 0.27$) by a power law corresponding to $\alpha = 1.94 \pm 0.06$ and $t_{min} = 0.20$ s. Corresponding off times are best fit to a log-normal distribution with $\mu = -0.17 \pm 0.09$, $\sigma = 0.92 \pm 0.07$, and $p = 0.67$. The observation of log-normally distributed off times for an individual molecule is consistent with a dispersive kinetics model for blinking that incorporates dynamic heterogeneity (i.e., rate constants that evolve in time).[48−51] Dispersive kinetics for an individual molecule have been reported in multi-chromophoric systems[50] as well as for molecules embedded within crystal[51] and polymer[31,52,53] environments, which provide enhanced stability. The present case is unusual in that dispersive kinetics are observed for an individual molecule on glass and in the presence of oxygen.

Overall, significant differences in single-molecule emission behavior are observed for EY in the presence and absence of oxygen. Many more blinking events are detected for EY in air as compared to N_2, as evidenced by an order of magnitude increase in the average single-molecule event rate. The on- and off-event durations are also significantly shorter in air relative to N_2. Furthermore, the majority of EY molecules in N_2 exhibited photobleaching within 200 s, but persistent blinking dynamics are observed for EY in air. Both on-time probability distributions are well-represented by power laws after an onset time, and modifications to α are observed for EY in N_2 (i.e., $\alpha = 2.46 \pm 0.03$) as compared to air (i.e., $\alpha = 2.38 \pm 0.02$). The best-fit parameters of the off-time probability distributions are significantly different for N_2 (i.e., $\mu = 1.64 \pm 0.08$ and $\sigma = 1.72 \pm 0.05$) relative to air (i.e., $\mu = 0.10 \pm 0.03$ and $\sigma = 1.07 \pm 0.02$). Altogether, oxygen plays a significant role in the emission dynamics of EY, consistent with a physical mechanism for blinking that involves population and depopulation of the triplet state.

DISCUSSION

Origin of Power-Law and Log-Normal Distributions. Previous studies have demonstrated that the observation of power-law and log-normal distributions is consistent with dispersive electron transfer between photoexcited dyes and a substrate (Figure 4A).[26] Here k_{exc} and k_{fl} are the rate constants for excitation and emission, respectively. The rate constants for population and depopulation of the dark state (i.e., for injection (k_{inj}) and recombination (k_{rec}), respectively) are not single-valued, consistent with a Gaussian distribution of activation barriers to electron transfer (i.e., the Albery model).[30] Within this three-electronic-state model for blinking, the off-event duration (τ_{off}) is equivalent to the dark-state lifetime (i.e., $\tau_{rec} = 1/k_{rec}$), and the Albery model predicts a log-normal distribution of off times. The lifetime of the emissive state in Figure 4A ($\tau_{on,A}$) is dependent on the rate constant for dark-state population (k_{inj}) and the fractional population of the singlet excited state according to

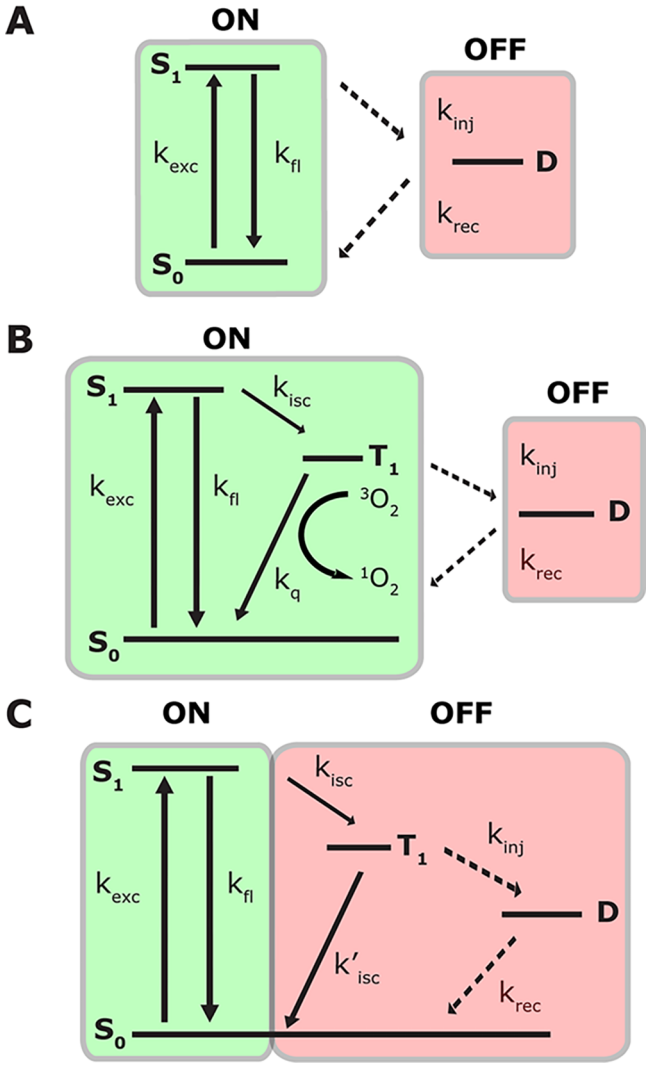

Figure 4. Schematic energy-level diagrams to account for blinking consisting of a singlet ground state (S_0), first excited singlet state (S_1), first excited triplet state (T_1), and a dark state (D), with corresponding rate constants: (A) dispersive electron transfer; triplet blinking and dispersive electron transfer in the (B) presence and (C) absence of oxygen.

$$\tau_{on,A} = \left[k_{inj} \left(\frac{k_{exc}}{k_{inj} + k_{fl}} \right) \right]^{-1} \quad (3)$$

Previous work has shown that, since the on-time probability distribution is a convolution of complex kinetics for emission and injection, on times can be power-law or log-normally distributed.[25,26,29] Thus, the observation of power-law and log-normal distributions for EY supports the role of dispersive electron transfer in the observed blinking dynamics. However, this interpretation is incomplete for two reasons: (1) the Albery model does not account for the observed oxygen-dependent photophysics of EY that are consistent with triplet-state blinking, and (2) fitting the off-time probability distributions yielded statistically insignificant results (i.e., p-values <0.05), suggesting that the log-normal distribution is an insufficient model for the data. These issues motivated us to investigate kinetic models that incorporate both triplet blinking and dispersive electron transfer.

DOI: 10.1021/acs.jpca.9b00409
J. Phys. Chem. A 2019, 123, 2592−2600

Kinetic Models for Triplet Blinking and Dispersive Electron Transfer. Previous single-molecule studies in polymer[45] and crystal[54] environments employed a four-state system involving a triplet state and a dark state to model power-law behavior. In the present case, both power-law and log-normal distributions are observed, albeit with relatively modest goodness-of-fit values. Figure 4B presents a proposed four-electronic-state system to account for the oxygen-dependent photophysics of EY and the observation of log-normal distributions. In this model, photoexcitation of EY to the first excited singlet state (S_1) is followed by rapid ISC to the triplet state (T_1), the latter of which is quenched by triplet oxygen ($^3O_2$) to produce singlet oxygen ($^1O_2$) with corresponding rate constant, k_q. If depopulation of T_1 via quenching is rapid relative to population of the triplet state via ISC, then a small steady-state concentration of T_1 is present, and the four-state system effectively reduces to a three-state system (Figure 4A). In this scenario, population of the dark state via dispersive electron transfer is likely to occur from S_1 (i.e., the reported redox potential of EY in the excited singlet state, E^0 (EY^*/EY^+), is −1.53 V)[7,55] to localized trap states in glass.[46]

In this approximation, τ_{off} is equivalent to the dark-state lifetime (i.e., τ_{rec}), and the off-time distribution is predicted to follow a log-normal distribution. Corresponding on times for the model in Figure 4B ($\tau_{on,B}$) are dependent on the rate constant for dark-state population (k_{inj}) and the fractional populations of the excited singlet and triplet states according to

$$\tau_{on,B} = \left[k_{inj} \left(\frac{k_{exc}}{k_{inj} + k_{fl}} \right) \left(\frac{k_{isc}}{k'_{isc} + k_{inj}} \right) \right]^{-1} \quad (4)$$

The on-time probability distribution is a convolution of the kinetics for emission as well as dark-state population and depopulation. Ultimately, rapid quenching of T_1 by oxygen effectively reduces the system to the three-state dispersive electron-transfer model for blinking (i.e., where "on" corresponds to $S_0 \rightleftarrows S_1$, and "off" is the nonemissive radical cation state of the dye).[7]

If, however, oxygen is not present or k_q is not sufficiently large as compared to k_{isc}, then a more complex picture emerges (Figure 4C). In this model, both triplet blinking and dispersive electron transfer are operative, such that the measured off times originate from both τ_{rec} and the lifetime of triplet state (i.e.,$\tau_T = 1/k'_{isc}$). Therefore, the off-time distribution is expected to be a convolution of an exponential distribution, consistent with first-order kinetics for triplet-state blinking, and a log-normal distribution corresponding to dispersive electron transfer from S_1 and/or T_1.[7] For the model in Figure 4C, on times ($\tau_{on,C}$) are dependent on the rate constant for ISC to the triplet state (k_{isc}) and the fractional population of the singlet excited state according to

$$\tau_{on,C} = \left[k_{isc} \left(\frac{k_{exc}}{k_{inj} + k_{fl}} \right) \right]^{-1} \quad (5)$$

Overall, the observation of complex on-time probability distributions that are not particularly well-represented by any of the tested functions is consistent with the models presented in Figure 4B,C. The observation that a log-normal distribution somewhat represents the off-time data for EY in N_2 suggests that the model in Figure 4C may be operative. In this case, the statistically insignificant p-value hints at the presence of more complex dynamics and an underlying onset time for log-normal behavior. However, the current MLE/KS method does not enable differentiation between competitive photophysical processes within an individual probability distribution (e.g., attempting to fit the data to an exponential distribution for triplet blinking and a log-normal distribution corresponding to dispersive electron transfer). To test the hypothesis that triplet-state decay contributes to the off-time probability distribution of EY in N_2, we explored fitting approaches that can be used to detect the competitive photophysics that may be underway.

Recently, Mitsui and co-workers developed a "scanning" MLE/KS method, where the onset time (t_{min}) of log-normal behavior is progressively changed to determine if the data contains contributions from other functions.[56] By calculating the p-value as a function of t_{min}, they demonstrated the off-time probability distribution of Atto 647N dyes on TiO_2 is well-described using a combination of exponential, power-law, and log-normal functions. An alternative approach, described by Clauset and co-workers,[27] uses the combined MLE/KS method to determine the best t_{min} such that the data are fit only where the log-normal distribution is operative. In this framework, the log-normal distribution is normalized from t_{min} (instead of zero as is done for eq 2) to yield

$$P(t) = \frac{1}{t} \sqrt{\frac{2}{\pi\sigma^2}} \left[\mathrm{erfc}\left(\frac{\ln(t_{min}) - \mu}{\sqrt{2}\sigma} \right) \right]^{-1} e^{-\left(\frac{(\ln(t)-\mu)^2}{2\sigma^2} \right)} \quad (6)$$

where μ and σ are the familiar log-normal fit parameters.

To explore the possibility that multiple processes contribute to the off-time probability distribution of EY in N_2, we examined the data using the approach where t_{min} is explicitly determined using MLE/KS as well as the scanning MLE/KS method. Figure S3 demonstrates the results of the scanning MLE/KS method. In this case, a value for t_{min} that is both statistically significant and physically relevant could not be unambiguously determined. Therefore, we shifted our approach to MLE/KS method, where the best t_{min} value is explicitly determined using eq 6. Figure 5 presents the best fit to the off-time probability distribution of EY in N_2 corresponding to a log-normal distribution with t_{min} = 0.14 s, $\mu = 1.63 \pm 0.06$, $\sigma = 1.8 \pm 0.1$, and $p = 0.07$. The p-value of 0.07 indicates that the log-normal distribution is a plausible model for the 98% of off times that occur after t_{min}. Likewise, the log-

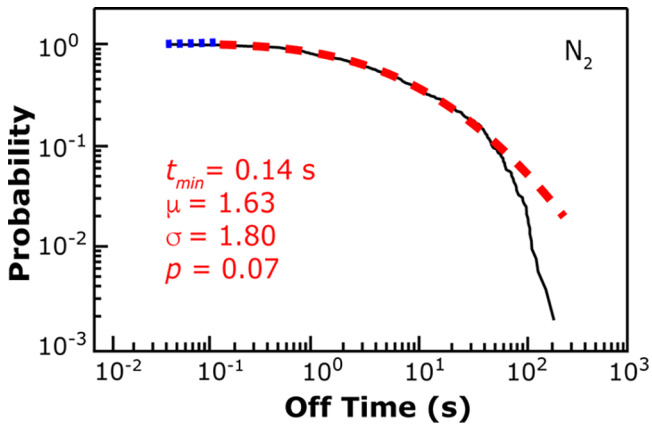

Figure 5. Off-time probability distribution (solid line) of EY in N_2 shown with best fit to an log-normal function after an onset time of 0.14 s (red dashed line) and an exponential function at early times (blue dotted line).

DOI: 10.1021/acs.jpca.9b00409
J. Phys. Chem. A 2019, 123, 2592−2600

normal distribution is not operative for off times shorter than 0.14 s, supporting the idea that these early time events originate from a different photophysical process such as triplet-state decay. Importantly, we examined all of the on- and off-time data for EY using this methodology, and no other distribution yielded a t_{min} value beyond the first data point (Table S1).

The observation that the off-time probability distributions for EY in N_2 is best fit to a log-normal function after an onset time is consistent with the kinetic model presented in Figure 4C. In the absence of oxygen, both triplet blinking and dispersive electron transfer are operative, such that the measured τ_{off} values contain contributions from both processes. Therefore, the off-time probability distribution is a convolution of an exponential distribution at early times, consistent with first-order kinetics for triplet-state blinking, and a log-normal distribution at later times corresponding to dispersive electron transfer from S_1 and/or T_1. It is possible that a power law could be used to represent the tail of the distribution (i.e., $>10^2$ s), consistent with the power-law fitting results presented in Table 1 (i.e., $\alpha = 6.7 \pm 0.3$, $t_{min} = 107.43$ s, and $p = 0.74$). However, the addition of a third function to fit the data is not justified, because (1) a statistically significant p-value for the log-normal distribution after t_{min} is observed and (2) its physical significance is unclear.

Figure 5 presents the best fit of the early off times (i.e., from 0.04 to 0.14 s) to an exponential decay (i.e., $P(t) = \frac{1}{\tau}e^{-t/\tau}$) corresponding to $\tau = 93$ ms. The time constant of the exponential decay is an order of magnitude longer than the reported 1 ms triplet lifetime of EY on alumina,[44] which indicates that triplet-state decay is occurring at time scales faster than the 10 ms integration time of the experiment. To test this hypothesis, we measured the blinking dynamics of EY using a 1 ms bin time, but the corresponding signal-to-noise ratios were too low to avoid the introduction of binning-induced artifacts to the data.[57,58] Nonetheless, extending the MLE/KS method to include an onset time for log-normal behavior provides for detection of early time contributions to the probability distribution that correspond to triplet-state decay.

Ultimately, the robust MLE/KS analysis of the on- and off-time probability distributions reveals the contributions of triplet-state decay and dispersive electron transfer to the excited-state dynamics of EY. In anoxic environment, both triplet-state decay and dispersive electron transfer from S_1 and/or T_1 contribute to the blinking dynamics of EY (Figure 4C). In oxic conditions T_1 is rapidly quenched by $^3O_2$ to produce $^1O_2$, and therefore, dispersive electron transfer from S_1 to traps on glass is predominately responsible for blinking (Figure 4B). The relationship between log-normal fit parameters and dispersive electron-transfer kinetics has been previously demonstrated, with $-\mu_{off}$ being proportional to the average rate constant for dark-state depopulation (i.e., $-\mu_{off} = \langle \ln(k_{off}) \rangle$) and σ_{off} proportional to the energetic dispersion around the mean activation barrier.[25] The observed $-\mu_{off}$ value of -0.10 ± 0.03 for EY in air is similar to the reported values for rhodamine dyes that do not possess heavy atoms,[26] further supporting the interpretation that triplet-state blinking of EY is not operative in the presence of oxygen. Finally, the observation that EY exhibits persistent blinking dynamics (i.e., rare photobleaching events) in oxic conditions is consistent with prior work and suggests that the short lifetime of $^1O_2$ and its rapid diffusion from the glass substrate limits the extent of oxidative degradation.[36]

Significant modifications to σ are observed for EY in air (i.e., $\sigma_{off} = 1.07 \pm 0.02$) as compared to N_2 (i.e., $\sigma_{off} = 1.8 \pm 0.1$), suggesting that different underlying processes contribute to kinetic dispersion in these environments. It is likely that both static and dynamic heterogeneity of electron transfer is operative, consistent with the observation of dispersive kinetics in an *individual molecule* of EY in air. Furthermore, temporal fluctuations to the triplet-state lifetime and fluorescence quantum yield due to spectral diffusion (e.g., during photo-induced debromination)[36] are also possible, consistent with the observation of multiple emissive intensities in the blinking dynamics of EY. These observations motivate further investigations to understand the role of spectral diffusion in the excited-state dynamics of EY.

CONCLUSION

We have used single-molecule spectroscopy to probe the extent and origin of kinetic dispersion in the excited-state dynamics of EY. By extending statistically principled approaches based on MLE/KS to quantify blinking dynamics in the presence and absence of oxygen, we discovered that both triplet-state decay and dispersive electron transfer are operative. The on-time probability distributions for EY in N_2 and air are power-law distributed after ~1 s, with fit parameters that are significantly modified upon exposure to oxygen. The off-time distribution for EY in N_2 is best fit to a combination of exponential and log-normal functions, consistent with a kinetic model that incorporates the competitive processes of triplet-state decay and dispersive electron transfer from S_1 and/or T_1 to trap states on glass. The corresponding off-time distribution for EY in air is best fit to a log-normal function alone, consistent with dispersive electron transfer from S_1. These observations support the role of static and dynamic heterogeneity in the electron-transfer dynamics, consistent with the observation of dispersive kinetics in an *individual molecule* of EY on glass. These measurements reveal the complex photophysical distributions of EY photosensitizers, providing new insights that are relevant to the design and development of next-generation materials for DSP, photoredox synthesis, and photodynamic therapy.

ASSOCIATED CONTENT

Supporting Information

The Supporting Information is available free of charge on the ACS Publications website at DOI: 10.1021/acs.jpca.9b00409.

> Blinking dynamics of a single EY molecule in air glass recorded over a long observation window; on- and off-time probability distributions for a single EY molecule; scanning MLE/KS analysis of the off-time probability distribution for EY in N_2; best-fit parameters and p-values for log-normal distributions with and without an onset time (PDF)

AUTHOR INFORMATION

Corresponding Author

*E-mail: kwustholz@wm.edu.

ORCID

Kristin L. Wustholz: 0000-0001-7705-4240

Notes

The authors declare no competing financial interest.

DOI: 10.1021/acs.jpca.9b00409
J. Phys. Chem. A 2019, 123, 2592−2600

Biography

Kristin Wustholz obtained a B.A.S. in chemistry and philosophy from Muhlenberg College. She received a Ph.D. in chemistry from the University of Washington studying single-molecule fluorescence in the laboratories of Philip J. Reid and Bart Kahr. Her research as a postdoctoral fellow at Northwestern University with Richard P. Van Duyne focused on single-molecule and single-nanoparticle SERS. Kristin joined the faculty at the College of William and Mary in 2010, where she is now the Class of 1964 Distinguished Associate Professor of Chemistry. Her research focuses on understanding the properties of chromophores near semiconductor and noble metal nanostructures for applications in solar energy conversion and chemical sensing.

■ ACKNOWLEDGMENTS

This work was supported by a grant from the National Science Foundation (CHE-1664828). We thank the Charles Center at the College of William and Mary for providing funding through an Honors fellowship to P.G.L. This work was performed in part using computing facilities at the College of William and Mary, which were provided by contributions from the National Science Foundation, the Commonwealth of Virginia Equipment Trust Fund and the Office of Naval Research.

■ REFERENCES

(1) Lewis, N. S.; Nocera, D. G. Powering the Planet: Chemical Challenges in Solar Energy Utilization. *Proc. Natl. Acad. Sci. U. S. A.* **2006**, *103*, 15729−15735.
(2) Caldeira, K.; Jain, A. K.; Hoffert, M. I. Climate Sensitivity Uncertainty and the Need for Energy without CO_2 Emission. *Science* **2003**, *299*, 2052−2054.
(3) Cook, T. R.; Dogutan, D. K.; Reece, S. Y.; Surendranath, Y.; Teets, T. S.; Nocera, D. G. Solar Energy Supply and Storage for the Legacy and Nonlegacy Worlds. *Chem. Rev.* **2010**, *110*, 6474−6502.
(4) Willkomm, J.; Orchard, K. L.; Reynal, A.; Pastor, E.; Durrant, J. R.; Reisner, E. Dye-Sensitised Semiconductors Modified with Molecular Catalysts for Light-Driven H_2 Production. *Chem. Soc. Rev.* **2016**, *45*, 9−23.
(5) Haque, S. A.; Palomares, E.; Cho, B. M.; Green, A. N. M.; Hirata, N.; Klug, D. R.; Durrant, J. R. Charge Separation Versus Recombination in Dye-Sensitized Nanocrystalline Solar Cells: The Minimization of Kinetic Redundancy. *J. Am. Chem. Soc.* **2005**, *127*, 3456−3462.
(6) Koops, S. E.; O'Regan, B. C.; Barnes, P. R. F.; Durrant, J. R. Parameters Influencing the Efficiency of Electron Injection in Dye-Sensitized Solar Cells. *J. Am. Chem. Soc.* **2009**, *131*, 4808−4818.
(7) Lazarides, T.; McCormick, T.; Du, P.; Luo, G.; Lindley, B.; Eisenberg, R. Making Hydrogen from Water Using a Homogeneous System Without Noble Metals. *J. Am. Chem. Soc.* **2009**, *131*, 9192−9194.
(8) Hartley, C. L.; DiRisio, R. J.; Screen, M. E.; Mayer, K. J.; McNamara, W. R. Iron Polypyridyl Complexes for Photocatalytic Hydrogen Generation. *Inorg. Chem.* **2016**, *55*, 8865−8870.
(9) Min, S.; Lu, G. Enhanced Electron Transfer from the Excited Eosin Y to mpg-C_3N_4 for Highly Efficient Hydrogen Evolution under 550 nm Irradiation. *J. Phys. Chem. C* **2012**, *116*, 19644−19652.
(10) Misawa, H. Photosensitizing Action of Eosin Y for Visible Light Induced Hydrogen Evolution from Water. *Chem. Lett.* **1983**, *12*, 1021−1024.
(11) Shimidzu, T.; Iyoda, T.; Koide, Y. An Advanced Visible-Light-Induced Water Reduction with Dye-Sensitized Semiconductor Powder Catalyst. *J. Am. Chem. Soc.* **1985**, *107*, 35−41.
(12) Wang, J.; Liu, Y.; Li, Y.; Xia, L.; Jiang, M.; Wu, P. Highly Efficient Visible-Light-Driven H_2 Production Via an Eosin Y-Based Metal−Organic Framework. *Inorg. Chem.* **2018**, *57*, 7495−7498.
(13) Hashimoto, K.; Kawai, T.; Sakata, T. The Mechanism of Photocatalytic Hydrogen Production with Halogenated Fluorescein Derivatives. *Nouv. J. Chim.* **1984**, *8*, 693−700.
(14) Hari, D. P.; König, B. Synthetic Applications of Eosin Y in Photoredox Catalysis. *Chem. Commun.* **2014**, *50*, 6688−6699.
(15) Srivastava, V.; Singh, P. P. Eosin Y Catalysed Photoredox Synthesis: A Review. *RSC Adv.* **2017**, *7*, 31377−31392.
(16) McNeil, I. J.; Ashford, D. L.; Luo, H. L.; Fecko, C. J. Power-Law Kinetics in the Photoluminescence of Dye-Sensitized Nanoparticle Films: Implications for Electron Injection and Charge Transport. *J. Phys. Chem. C* **2012**, *116*, 15888−15899.
(17) Grollman, R.; Quist, N.; Robertson, A.; Rath, J.; Purushothaman, B.; Haley, M. M.; Anthony, J. E.; Ostroverkhova, O. Single-Molecule Level Insight Into Nanoscale Environment-Dependent Photophysics in Blends. *J. Phys. Chem. C* **2017**, *121*, 12483−12494.
(18) Guo, L.; Wang, Y.; Lu, H. P. Combined Single-Molecule Photon-Stamping Spectroscopy and Femtosecond Transient Absorption Spectroscopy Studies of Interfacial Electron Transfer Dynamics. *J. Am. Chem. Soc.* **2010**, *132*, 1999−2004.
(19) Wu, X. Y.; Bell, T. D. M.; Yeow, E. K. L. Electron Transport in the Long-Range Charge-Recombination Dynamics of Single Encapsulated Dye Molecules on TiO_2 Nanoparticle Films. *Angew. Chem., Int. Ed.* **2009**, *48*, 7379−7382.
(20) Wang, Y. M.; Wang, X. F.; Ghosh, S. K.; Lu, H. P. Probing Single-Molecule Interfacial Electron Transfer Dynamics of Porphyrin on TiO_2 Nanoparticles. *J. Am. Chem. Soc.* **2009**, *131*, 1479−1487.
(21) Biju, V.; Micic, M.; Hu, D. H.; Lu, H. P. Intermittent Single-Molecule Interfacial Electron Transfer Dynamics. *J. Am. Chem. Soc.* **2004**, *126*, 9374−9381.
(22) Godin, R.; Sherman, B. D.; Bergkamp, J. J.; Chesta, C. A.; Moore, A. L.; Moore, T. A.; Palacios, R. E.; Cosa, G. Charge-Transfer Dynamics of Fluorescent Dye-Sensitized Electrodes under Applied Biases. *J. Phys. Chem. Lett.* **2015**, *6*, 2688−2693.
(23) Sevinc, P. C.; Dhital, B.; Govind Rao, V.; Wang, Y.; Lu, H. P. Probing Electric Field Effect on Covalent Interactions at a Molecule−Semiconductor Interface. *J. Am. Chem. Soc.* **2016**, *138*, 1536−1542.
(24) Rao, V.; Dhital, B.; Peter Lu, H. Single-Molecule Interfacial Electron Transfer Dynamics of Porphyrin on TiO_2 Nanoparticles: Dissecting the Interfacial Electric Field and Electron Accepting State Density Dependent Dynamics. *Chem. Commun.* **2015**, *51*, 16821−16824.
(25) Tan, J. A.; Rose, J. T.; Cassidy, J. P.; Rohatgi, S. K.; Wustholz, K. L. Dispersive Electron-Transfer Kinetics of Rhodamines on TiO_2: Impact of Structure and Driving Force on Single-Molecule Photophysics. *J. Phys. Chem. C* **2016**, *120*, 20710−20720.
(26) Wong, N. Z.; Ogata, A. F.; Wustholz, K. L. Dispersive Electron-Transfer Kinetics from Single Molecules on TiO_2 Nanoparticle Films. *J. Phys. Chem. C* **2013**, *117*, 21075−21085.
(27) Clauset, A.; Shalizi, C.; Newman, M. Power-Law Distributions in Empirical Data. *SIAM Rev.* **2009**, *51*, 661−703.
(28) Riley, E. A.; Hess, C. M.; Whitham, P. J.; Reid, P. J. Beyond Power Laws: A New Approach for Analyzing Single Molecule Photoluminescence Intermittency. *J. Chem. Phys.* **2012**, *136*, 10.

DOI: 10.1021/acs.jpca.9b00409
J. Phys. Chem. A 2019, 123, 2592−2600

(29) Tan, J. A.; Garakyaraghi, S.; Tagami, K. A.; Frano, K. A.; Crockett, H. M.; Ogata, A. F.; Patterson, J. D.; Wustholz, K. L. Contributions from Excited-State Proton and Electron Transfer to the Blinking and Photobleaching Dynamics of Alizarin and Purpurin. *J. Phys. Chem. C* **2017**, *121*, 97−106.
(30) Albery, W. J.; Bartlett, P. N.; Wilde, C. P.; Darwent, J. R. A General-Model for Dispersed Kinetics in Heterogeneous Systems. *J. Am. Chem. Soc.* **1985**, *107*, 1854−1858.
(31) Mitsui, M.; Unno, A.; Azechi, S. Understanding Photoinduced Charge Transfer Dynamics of Single Perylenediimide Dyes in a Polymer Matrix by Bin-Time Dependence of Their Fluorescence Blinking Statistics. *J. Phys. Chem. C* **2016**, *120*, 15070−15081.
(32) Amat-Guerri, F.; López-González, M. M. C.; Martínez-Utrilla, R.; Sastre, R. Singlet Oxygen Photogeneration by Ionized and Un-Ionized Derivatives of Rose Bengal and Eosin Y in Diluted Solutions. *J. Photochem. Photobiol., A* **1990**, *53*, 199−210.
(33) Niedre, M.; Patterson, M. S.; Wilson, B. C. Direct Near-Infrared Luminescence Detection of Singlet Oxygen Generated by Photodynamic Therapy in Cells in Vitro and Tissues in Vivo. *Photochem. Photobiol.* **2002**, *75*, 382−391.
(34) Casadio, F.; Leona, M.; Lombardi, J. R.; Van Duyne, R. Identification of Organic Colorants in Fibers, Paints, and Glazes by Surface Enhanced Raman Spectroscopy. *Acc. Chem. Res.* **2010**, *43*, 782−791.
(35) Centeno, S. A.; Hale, C.; Carò, F.; Cesaratto, A.; Shibayama, N.; Delaney, J.; Dooley, K.; van der Snickt, G.; Janssens, K.; Stein, S. A. Van Gogh's Irises and Roses: the Contribution of Chemical Analyses and Imaging to the Assessment of Color Changes in the Red Lake Pigments. *Heritage Sci.* **2017**, *5*, 18.
(36) Alvarez-Martin, A.; Trashin, S.; Cuykx, M.; Covaci, A.; De Wael, K.; Janssens, K. Photodegradation Mechanisms and Kinetics of Eosin-Y in Oxic and Anoxic Conditions. *Dyes Pigm.* **2017**, *145*, 376−384.
(37) Watkins, L. P.; Yang, H. Detection of Intensity Change Points in Time-Resolved Single-Molecule Measurements. *J. Phys. Chem. B* **2005**, *109*, 617−628.
(38) Bott, E. D.; Riley, E. A.; Kahr, B.; Reid, P. J. Proton-Transfer Mechanism for Dispersed Decay Kinetics of Single Molecules Isolated in Potassium Hydrogen Phthalate. *ACS Nano* **2009**, *3*, 2403−2411.
(39) Wustholz, K. L.; Bott, E. D.; Kahr, B.; Reid, P. J. Memory and Spectral Diffusion in Single-Molecule Emission. *J. Phys. Chem. C* **2008**, *112*, 7877−7885.
(40) Riley, E. A.; Bingham, C.; Bott, E. D.; Kahr, B.; Reid, P. J. Two Mechanisms for Fluorescence Intermittency of Single Violamine R Molecules. *Phys. Chem. Chem. Phys.* **2011**, *13*, 1879−1887.
(41) Bott, E. D.; Riley, E. A.; Kahr, B.; Reid, P. J. Unraveling the Dispersed Kinetics of Dichlorofluorescein in Potassium Hydrogen Phthalate Crystals. *J. Phys. Chem. A* **2010**, *114*, 7331−7337.
(42) Nishimura, Y. Xanthene Dye-Sensitized Electron Transfer to Methylviologen in Aqueous Organic Solution. Effects of Organic Solvents and Heavy Atoms in the Dyes. *Bull. Chem. Soc. Jpn.* **1992**, *65*, 2887−2893.
(43) Garland, P. B.; Moore, C. H. Phosphorescence of Protein-Bound Eosin and Erythrosin. A Possible Probe for Measurements of Slow Rotational Mobility. *Biochem. J.* **1979**, *183*, 561−572.
(44) Levin, P. P.; Costa, S. M. Kinetics of Oxygen Induced Delayed Fluorescence of Eosin Adsorbed on Alumina. The Dependence on Dye and Oxygen Concentrations. *Chem. Phys. Lett.* **2000**, *320*, 194−201.
(45) Zondervan, R.; Kulzer, F.; Orlinskii, S. B.; Orrit, M. Photoblinking of Rhodamine 6g in Poly(Vinyl Alcohol): Radical Dark State Formed through the Triplet. *J. Phys. Chem. A* **2003**, *107*, 6770−6776.
(46) Yeow, E. K. L.; Melnikov, S. M.; Bell, T. D. M.; De Schryver, F. C.; Hofkens, J. Characterizing the Fluorescence Intermittency and Photobleaching Kinetics of Dye Molecules Immobilized on a Glass Surface. *J. Phys. Chem. A* **2006**, *110*, 1726−1734.
(47) Penzkofer, A.; Beidoun, A.; Daiber, M. Intersystem-Crossing and Excited-State Absorption in Eosin Y Solutions Determined by Picosecond Double Pulse Transient Absorption Measurements. *J. Lumin.* **1992**, *51*, 297−314.
(48) Kuno, M.; Fromm, D. P.; Johnson, S. T.; Gallagher, A.; Nesbitt, D. J. Modeling Distributed Kinetics in Isolated Semiconductor Quantum Dots. *Phys. Rev. B: Condens. Matter Mater. Phys.* **2003**, *67*, 125304.
(49) Pelton, M.; Grier, D. G.; Guyot-Sionnest, P. Characterizing Quantum-Dot Blinking Using Noise Power Spectra. *Appl. Phys. Lett.* **2004**, *85*, 819−821.
(50) Hoogenboom, J. P.; van Dijk, E.; Hernando, J.; van Hulst, N. F.; Garcia-Parajo, M. F. Power-Law-Distributed Dark States Are the Main Pathway for Photobleaching of Single Organic Molecules. *Phys. Rev. Lett.* **2005**, *95*, 097401.
(51) Wustholz, K. L.; Bott, E. D.; Isborn, C. M.; Li, X.; Kahr, B.; Reid, P. J. Dispersive Kinetics from Single Molecules Oriented in Single Crystals of Potassium Acid Phthalate. *J. Phys. Chem. C* **2007**, *111*, 9146−9156.
(52) Clifford, J. N.; Bell, T. D. M.; Tinnefeld, P.; Heilemann, M.; Melnikov, S. M.; Hotta, J.; Sliwa, M.; Dedecker, P.; Sauer, M.; Hofkens, J.; et al. Fluorescence of Single Molecules in Polymer Films: Sensitivity of Blinking to Local Environment. *J. Phys. Chem. B* **2007**, *111*, 6987−6991.
(53) Rao, V.; Dhital, B.; He, Y.; Lu, H. P. Single-Molecule Interfacial Electron Transfer Dynamics of Porphyrin on TiO_2 Nanoparticles: Dissecting the Complex Electronic Coupling Dependent Dynamics. *J. Phys. Chem. C* **2014**, *118*, 20209−20221.
(54) Barbon, A.; Bott, E. D.; Brustolon, M.; Fabris, M.; Kahr, B.; Kaminsky, W.; Reid, P. J.; Wong, S. M.; Wustholz, K. L.; Zanre, R. Triplet States of the Nonlinear Optical Chromophore Dcm in Single Crystals of Potassium Hydrogen Phthalate and Their Relationship to Single-Molecule Dark States. *J. Am. Chem. Soc.* **2009**, *131*, 11548−11557.
(55) Yin, M.; Li, Z.; Kou, J.; Zou, Z. Mechanism Investigation of Visible Light-Induced Degradation in a Heterogeneous TiO_2/Eosin Y/Rhodamine B System. *Environ. Sci. Technol.* **2009**, *43*, 8361−8366.
(56) Mitsui, M.; Unno, A.; Mori, K. Methodology for Discriminating between Competitive Photophysical Processes in Photoblinking: Application to the Fluorescence Blinking of Single Dye Molecules Adsorbed on TiO_2. *Chem. Lett.* **2017**, *46*, 866−869.
(57) Crouch, C. H.; Sauter, O.; Wu, X.; Purcell, R.; Querner, C.; Drndic, M.; Pelton, M. Facts and Artifacts in the Blinking Statistics of Semiconductor Nanocrystals. *Nano Lett.* **2010**, *10*, 1692−1698.
(58) Amecke, N.; Heber, A.; Cichos, F. Distortion of Power Law Blinking with Binning and Thresholding. *J. Chem. Phys.* **2014**, *140*, 114306.

DOI: 10.1021/acs.jpca.9b00409
J. Phys. Chem. A 2019, 123, 2592−2600